Supersaturation of Vertically Propagating Internal Gravity Waves

RICHARD S. LINDZEN

Center for Meteorology and Physical Oceanography, Massachusetts Institute of Technology, Cambridge, Massachusetts

(Manuscript received 18 May 1987, in final form 19 August 1987)

ABSTRACT

The usual assumption that vertically propagating internal gravity waves will cease growing with height once their amplitudes are such as to permit convective instability anywhere within the wave is reexamined. Two factors lead to amplitude limitation:

(i) wave clipping associated with convective mixing, and
(ii) energetic constraints associated with the rate at which the wave can supply energy to the convection.

It is found that these two factors limit supersaturation to about 50% for waves with short horizontal wavelengths and high relative phase speeds. Usually the degree of supersaturation will be much less. These factors also lead to a gradual, rather than sudden, cessation of wave growth with height.

1. Introduction

The general approach to gravity wave saturation over the years has been to assume that, once gravity waves reached an amplitude for which lapse rates (due to the sum of the mean state and the gravity wave perturbations) equalled the adiabatic lapse rate (beyond which there would be local convective instability), further wave growth would be suppressed (Lindzen, 1967, 1968, 1981; Lindzen and Blake, 1971; Hodges, 1968). This specific amplitude is called the saturation amplitude. Of course, it was realized that amplitudes would have to be greater than this (i.e., supersaturated) to actually maintain the convection, but it was assumed that this excess amplitude would be negligibly small.[1] The present paper attempts to assess this contention in a simple but systematic manner. Our approach is twofold:

(i) We explicitly consider the wave clipping due to convective mixing and its role in attenuating wave amplitudes[2]; and

(ii) We require that the rate of generation of convective motions in an unstable region be compatible with the rate at which the breaking wave is supplying energy to that region.

Superficially, the first aspect appears to allow substantial supersaturation, but the second aspect is much more constraining. Nevertheless, we find that fast [c (horizontal phase speed) $\geqslant 50$ m s^{-1}], short ($2\pi/k \leqslant 100$ km) waves can supersaturate moderately, though slower, longer waves do not. Even modest supersaturation, however, can significantly modify such things as the vertical distribution of mean stress due to breaking waves.

For purposes of simplicity and illustration we will consider a monochromatic internal gravity wave of specified frequency, σ (or phase speed c), and horizontal wavenumber, k, propagating through a static (or constant U), isothermal basic flow (characterized by $T = \bar{T}$) with a scale height $H = R\bar{T}/g$. Saturation will occur in this simple situation due to the growth of wave fields as $e^{z/2H}$ where z is height. Supersaturation will lead to wave "flattening" which will reduce the projection of the flattened wave on the original wavenumber. The

[1] In this regard, it is sometimes argued that it is Ri < 0.25 (where Richardson number $\mathrm{Ri} = N^2/(U_z^2)$; N is Brunt–Väisälä frequency based on the sum of the wave and the mean state; U_z is vertical shear of the total horizontal velocity) rather than Ri < 0 (i.e., $N^2 < 0$) which is the relevant instability criterion. However, for 0 < Ri < 0.25, instabilities do not necessarily set on (Lindzen and Barker, 1985) and when instabilities do set on, their growth rates are usually much smaller than for Ri < 0. For thin unstable layers, this is readily demonstrated by means of the semicircle theorems (Howard, 1961). We will therefore stick with the convective criterion.

[2] "Clipping" generally refers to a process that restricts the excursions of a sinusoidal oscillation to a value less than the oscillation's full amplitude—thus clipping the oscillation. Frequently this clipping applies only to the maximum positive excursion. As a result of convective instability, excursions of $-\partial\delta T/\partial z$ (where δT is the temperature perturbation associated with the wave and z is height) are restricted to $\Gamma \equiv d\bar{T}/dz + g/c_p$ ($\bar{T}$ is the basic state temperature, g is the acceleration of gravity, and c_p is the heat capacity of air at constant pressure). Such clipping is indicated in Fig. 1d. The consequences of such convective clipping for oscillations in δT at a particular level is flattening of the sort shown in Fig. 1b. The terms "clipping" and "flattening" will always be used in these senses.

Corresponding author address: Dr. Richard S. Lindzen, Center for Meteorology and Physical Oceanography, MIT, Cambridge, MA 02139.

degree of reduction increases with the degree of supersaturation. The equilibrated degree of supersaturation occurs when the amplitude reduction balances the $e^{z/2H}$ growth. In section 2 we describe in detail the implementation of this scheme. Our implementation will incorporate the constraint that unstable convective growth rates be bounded by the travel times for the waves to cross the unstable regions. The latter is a simple approach to energetic consistency for the wave driven convection. [Weinstock (1986) takes a similar but more elaborate approach to a simpler configuration.]

2. Mathematical development

For the simple situation described, the temperature perturbation associated with an unsaturated internal gravity wave will be of the form

$$\delta T \approx A \exp\left(i \int \lambda dz\right) \exp(z/2H) \exp[ik(x - ct)]. \quad (1)$$

The contribution of (1) to the total vertical temperature gradient is

$$\frac{d\delta T}{dz} \approx i\lambda A \exp\left(i \int \lambda dz\right) \exp(z/2H) \quad (2)$$

where we assume $\lambda \gg 1/2H$. Let the ambient static stability be given by

$$\Gamma = \frac{d\bar{T}}{dz} + \frac{g}{c_p}. \quad (3)$$

Finally, if we let

$$A = \frac{\Gamma}{\lambda} \tilde{A}, \quad (4)$$

the condition for saturation is simply

$$|\tilde{A}| = 1, \quad (5)$$

and (2) becomes

$$\frac{d\delta T}{dz} \approx i\Gamma\tilde{A} \exp\left(i \int \lambda dz\right) \exp(z/2H). \quad (6)$$

In the event of supersaturation, the maximum unstable local lapse rate is given by

$$(|\tilde{A}| - 1)\Gamma.$$

In the neighborhood of the maximum unstable lapse rate, the maximum growth rate for convective instabilities is given by

$$\sigma_c \approx \left(\frac{g}{T}(|\tilde{A}| - 1)\Gamma\right)^{1/2} \approx N(|\tilde{A}| - 1)^{1/2} \quad (7)$$

(see Appendix). When this convection sets on, the situation we envisage is as follows: In Fig. 1a we see a vertical section of δT; the region of depth D is statically unstable. The convection which occurs in region D will mix potential temperature. This, in turn, will lead to a smoothing of temperature over some region of horizontal length X displayed in the horizontal section shown in Fig. 1b. The relation between D and X will soon be discussed at length, but the overall situation is depicted in Fig. 1c, which schematically illustrates isentropic contours in the z–x plane with the region of expected convective mixing shaded. The continued growth of the wave (here associated with basic density diminishing with height) beyond saturation leads to the broadening of the convective wedge shown in Fig. 1c.

Now the "flattening" of the temperature in Fig. 1b will reduce the projection of the temperature variation on the original wave. The amplitude reduction of the projection is given by

$$f(a) = (1/\pi)\left\{\int_0^a + \int_{2\pi-a}^{2\pi} \sin^2 x dx\right\} \quad (8a)$$

$$= \frac{a - \frac{1}{2}\sin 2a}{\pi} \quad (8b)$$

where $a = \pi - k(X/2)$. Let $x = k(X/2)$, then

$$f(x) = \frac{(\pi - x) - \frac{1}{2}\sin 2(\pi - x)}{\pi}$$

$$= \frac{(\pi - x) + \frac{1}{2}\sin 2x}{\pi}. \quad (9)$$

It is easily seen that $0.5 \leq f(x) \leq 1$ (since $0 \leq x \leq \pi/2$). Presumably, the reduction associated with $f(x)$ competes with $\exp(z/2H)$ growth over some vertical scale proportional to D (as shown in Fig. 1a).

It is obvious that such flattening as may occur in reality cannot be as perfect as that shown in Fig. 1b (or assumed in the preceding analysis). However, as we will soon see, uncertainties as to what D is and as to whether D is the appropriate scale for $e^{z/2H}$ growth render a more careful approach to the question of flattening unwarranted.

Intuitively, we expect that D is related to X by the dispersion relation for internal gravity waves: i.e.,

$$l^2 \approx \frac{N^2}{\sigma^2} k^2$$

where $\sigma = kc$ is the wave frequency, and l = vertical wavenumber. Similarly,

$$D = \frac{\sigma}{N} X. \quad (10)$$

As already mentioned, it is unclear (even unlikely) that D is the appropriate scale for the $e^{z/2H}$ growth with which the clipping is competing. Such a supposition is largely based on "clipping" being the primary inhibiting process resulting from convection. Figure 1 implicitly relates to an unstable wave field which is set up at all levels before breaking down. It seems likely, however, that the convection also directly inhibits vertical propagation. To crudely account for this, we will assume

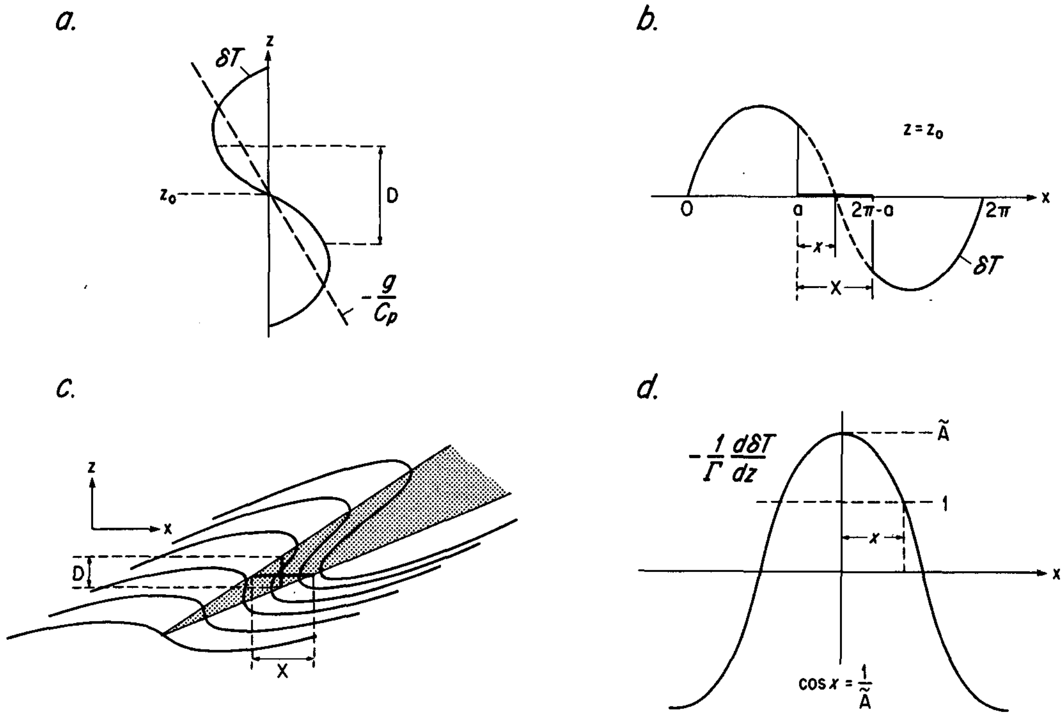

FIG. 1. Schematic depiction of a supersaturated wave. (a) δT vs z at a particular x; supersaturation occurs in region D. (b) δT vs x at a particular z; X is the region of convective mixing where "clipping" is introduced. (c) Isentropes (in the x–z plane) deformed by a supersaturated gravity wave; convective instability occurs in the shaded region. (d) Region of supersaturation as a function of x at a constant z level.

that the appropriate scale for $e^{z/2H}$ growth, D_g, is proportional to D:

$$D_g = \mu D \tag{11}$$

where μ (presumably <1) parameterizes the inhibiting effects of convective breaking on propagation. We will later pin down μ by insisting that in the presence of supersaturation, convective time scales are not shorter than travel times for the wave to travel through the convective region. In view of (11), the exponential growth factor is

$$g(X) = \exp(D_g/2H) = \exp\left(\mu \frac{\sigma}{N}\frac{X}{2H}\right). \tag{12}$$

For stationary waves (i.e., mountain waves) $\sigma = kU$ (for simple internal gravity waves in a nonrotating system there is no problem in replacing a static basic state with a constant flow, U). For $U \leqslant 50$ m s^{-1} and $\mu = 1$, it is easy to show that $g(X) < 1.5$ so that equilibration between g and f is possible. For $\mu < 1$, U can be much larger than 50 m s^{-1}. Using $\sigma = kU$, (12) becomes

$$g(X) = \exp\left(\mu \frac{kU}{N}\frac{X}{2H}\right);$$

or, using $(kX/2) = x$,

$$g(x) = \exp\left(\mu \frac{Ux}{NH}\right).$$

The net change of amplitude over depth D_g (when $|A| > 1$) is given by

$$F(x) = f(x)g(x). \tag{13}$$

Moreover, for $|\tilde{A}| > 1$ it is readily shown that

$$x = \cos^{-1}(1/\tilde{A}) \quad \text{(viz. Fig. 1d).} \tag{14}$$

Note that if one wishes to use (13) to calculate the change of amplitude over an arbitrary depth rather than over D_g, one proceeds as follows. First calculate the equivalent exponential growth factor over depth D_g:

$$F(x) = \exp(\lambda D_g);$$

then solve for λ:

$$\lambda = \frac{\ln F}{D_g};$$

and use

$$e^{\lambda z}$$

for the local growth of the amplitude. Later we will use this approach in order to calculate $\tilde{A}(z)$. For the moment, however, we will focus on the equilibrated value of $\tilde{A}$; i.e., that value for which $F(x) = 1$. It is, of course, a straightforward matter to solve for this value of x numerically (it will depend on $\mu U/NH$), and use (14) to obtain $\tilde{A}$. However, as we will show, the analytic approximation obtained next is almost always completely adequate.

For small x,

$$\sin x \approx x - (1/6)x^3,$$

and using (9),

$$f(x) \approx 1 - (2/3\pi)x^3.$$

Similarly,

$$g(x) \approx 1 + \frac{\mu U x}{NH}$$

$$F = fg \approx 1 - \frac{2}{3\pi}x^3 + \frac{\mu U x}{NH}.$$

Now $F(x_e) = 1$ (the subscript, e, refers to equilibration) implies

$$\frac{2}{3\pi}x_e^2 \approx \frac{\mu U}{NH},$$

or

$$x_e \approx \left(\frac{3\pi}{2}\frac{\mu U}{NH}\right)^{1/2}. \tag{15}$$

Finally,

$$\cos x_e \approx 1 - \frac{x_e^2}{2} \approx 1 - \frac{1}{2}\frac{3\pi}{2}\frac{\mu U}{NH},$$

$$\tilde{A}_e = \frac{1}{\cos x_e} \approx 1 + \frac{1}{2}\frac{3\pi}{2}\frac{\mu U}{NH}. \tag{16}$$

The last step in this procedure is the estimation of μ. As already noted, if we were to ignore all effects of convection other than clipping, then $\mu = 1$ would be a plausible choice. With this choice, (16) yields

$$\tilde{A}_e - 1 \approx \frac{3\pi}{4}\frac{U}{NH}. \tag{17}$$

Taking $N = 2\pi/300$ s, and $H = 7 \times 10^3$ m, we get

$$\tilde{A}_e - 1 \approx \frac{U}{62 \text{ m s}^{-1}} \leqslant 1. \tag{18}$$

This, in general, limits supersaturation to a factor typically less than 2. However, even this degree of supersaturation suffers (as we will show) from the defect that it leads to convective growth rates faster than the wave travel time across the convective region; i.e., the wave cannot supply the energy called for by the convection. In assessing this, there remains some ambiguity. In particular, do we calculate the travel time across D or D_g? The former choice would limit supersaturation more severely, but the latter choice seems intuitively more appropriate.

The vertical group velocity for our simple gravity wave is

$$c_G \approx \frac{kU^2}{N}, \tag{19}$$

and, for the equilibrated wave amplitude, D_g, is given by

$$D_g \approx \frac{2\mu U x_e}{N}, \tag{20}$$

so that the travel time across D_g is

$$\text{travel time} \approx \frac{D_g}{c_g} \approx \frac{2\mu U}{N}\left(\frac{3\pi}{2}\frac{\mu U}{NH}\right)^{1/2}\frac{N}{kU^2} \approx 2\mu\left(\frac{3\pi}{2}\frac{\mu U}{NH}\right)^{1/2}\frac{1}{kU}. \tag{21}$$

Using (7) and (16), the convective time scale is given by

$$\sigma_c^{-1} \approx N^{-1}\left(\frac{3\pi}{4}\frac{\mu U}{NH}\right)^{-1/2}.$$

Requiring that travel time $\approx \sigma_c^{-1}$ yields

$$\mu \approx \left(\frac{\sqrt{2}kH}{3\pi}\right)^{1/2} \approx \left(\frac{2\sqrt{2}}{3}\frac{H}{\text{hwl}}\right)^{1/2}. \tag{22}$$

For the most part, horizontal wave length, hwl $\geqslant 70$ km so that $\mu \leqslant 1/3$. Larger values of μ would lead to convective times which would be much shorter than the travel times across D_g (which are, in turn, shorter than those across D).

Using (22), (16) becomes

$$\tilde{A}_e \approx 1 + \frac{3\pi}{4}\frac{U}{NH}\left(\frac{\sqrt{2}kH}{3\pi}\right)^{1/2} \tag{23}$$

or

$$\tilde{A}_e \approx 1 + \frac{U}{4N}\left(\frac{3\pi\sqrt{2}k}{H}\right)^{1/2}. \tag{24}$$

While more detailed numerical results will be presented in the next section, a few quick estimates show the degree of supersaturation allowed by these considerations. Let $N \approx \frac{2\pi}{300 \text{ s}}$, and $H \approx 7 \times 10^3$ m. For $U \approx 20$ m s^{-1} and $k \approx \frac{2\pi}{1000 \text{ km}}$,

$$\tilde{A}_e - 1 \approx 0.025,$$

while for $U \approx 50$ m s^{-1} and $k \approx \frac{2\pi}{100 \text{ km}}$,

$$\tilde{A}_e - 1 \approx 0.2.$$

3. Numerical results

Quite clearly, if our "small x" approximation is adequate, it is a trivial matter to evaluate $\tilde{A}_e$ as a function of U, N and k (for stationary waves) or more generally as a function of U, σ, N and k. Thus, our first task is to compare exact and approximate evaluations of $\tilde{A}_e$ in order to show that this is, in fact, the case. Figure 2 shows such comparisons. We see that for ν $(=\mu\sigma/NH)$ > 0.2 the small x approximation becomes inaccurate. However, for $U = 75$ m s^{-1} and $k = 2\pi/40$ km, $\nu = 0.2$. For more typical longer wavelengths and smaller U, we have still smaller ν, and for such ν the small x approximation is excellent.

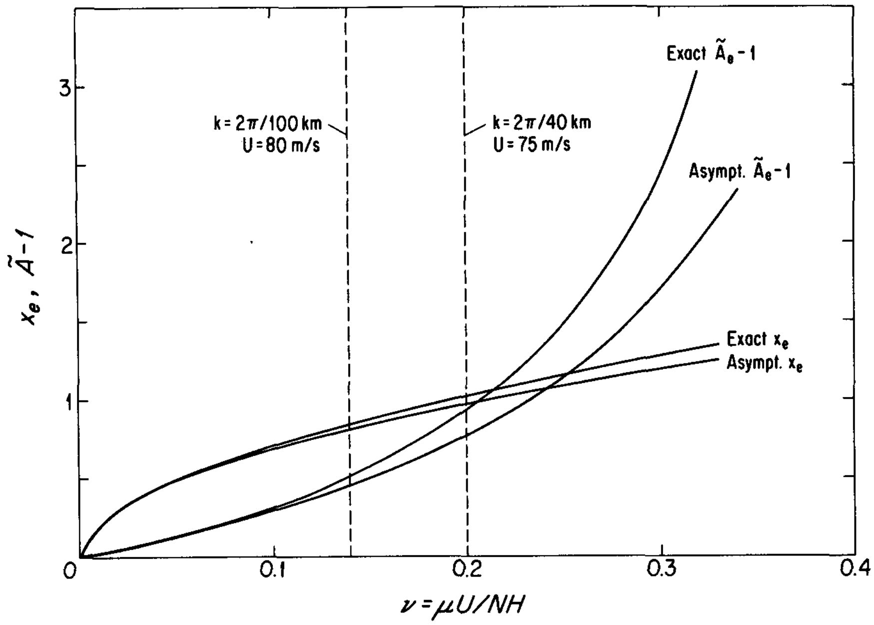

FIG. 2. Equilibrated values of A and x (i.e., A_e and x_e) as functions of $\nu = (\mu U/NH)$. N.B. $x_{e,\text{asymptotic}}$ is calculated using Eq. (15), while $A_{e,\text{ asymptotic}} = 1/(\cos x_{e,\text{asymptotic}})$. See text for details.

The evaluation of the vertical distribution of $\tilde{A}(z)$, showing how $\tilde{A}(z)$ approaches $\tilde{A}_e$, requires numerical evaluation. The curves in Fig. 3 were obtained following the procedure outlined in section 2. We see that for typical values of U and $2\pi/k$ (i.e., 30 m s^{-1} and 400 km, and 30 m s^{-1} and 100 km), $\tilde{A}_e - 1$ is small, and $\tilde{A}_e$ is reached within 1–4 km of the height at which wavebreaking begins. For more extreme values of U and $2\pi/k$ (40 m s^{-1} and 35 km, and 80 m s^{-1} and 100 km) we have modest supersaturation and it takes more than 10 km for $\tilde{A}(z)$ to reach $\tilde{A}_e$. In all cases, the approach to $\tilde{A}_e$ is smooth rather than abrupt.

Perhaps more important than $A(z)$, is the vertical distribution of $(\rho_0 uw)_z$, the acceleration of the mean flow by the breaking gravity wave. For the present simple case,

$$\text{acc} = (\rho_0 uw)_z/\rho_0 \propto e^{z/H}(A^2 e^{-z/H}). \tag{25}$$

Prior to breaking, $A \propto e^{z/2H}$, and $(\rho_0 uw)_z = 0$. Where A = constant, $e^{z/H}(A^2 e^{-z/H})_z = -A^2/H$, corresponding to uniform acceleration. In the simple models of breaking waves, mean flow acceleration sets on suddenly when the wave breaks (this is not the case, however, in Lindzen and Forbes, 1982, where neutral waves are assumed to generate low-level turbulence) and continues at a constant value (if U is taken to be independent of height) above the breaking level. Figure 4 shows the vertical distribution of acceleration for the cases considered in Fig. 3. We see that the effect of supersaturation on acceleration is more substantial than the effect on A alone (this is hardly surprising since acceleration $\propto A^2$). We see that for common val-

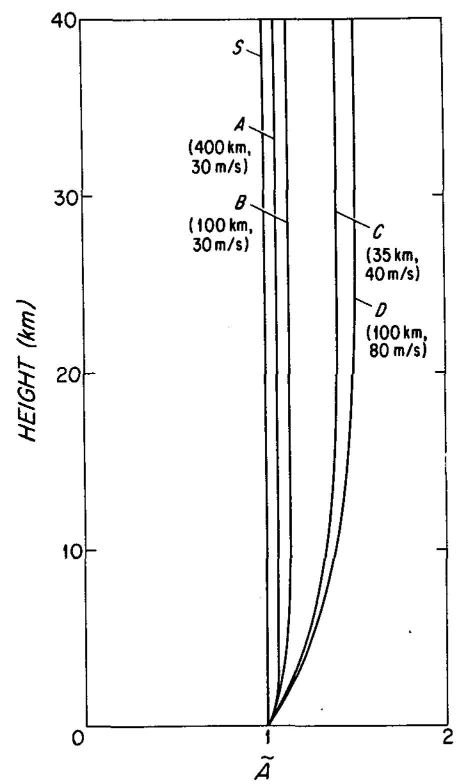

FIG. 3. A vs z. The line, S, corresponds to the simple model of Lindzen (1981), while the remaining curves are based on the present supersaturation model. A corresponds to $k = 2\pi/400$ km and U = 30 m s^{-1}; B corresponds to $k = 2\pi/100$ km and U = 30 m s^{-1}; C corresponds to $k = 2\pi/35$ km and U = 40 m s^{-1}; and D corresponds to $k = 2\pi/100$ km and U = 80 m s^{-1}.

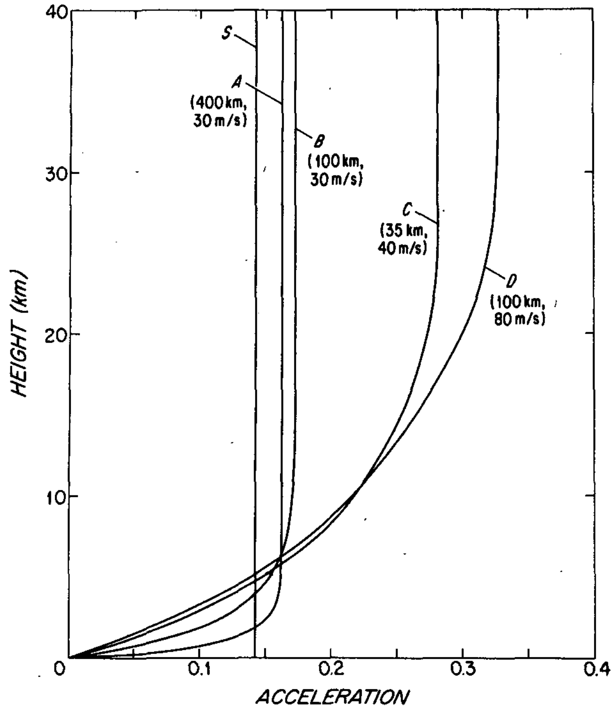

FIG. 4. Acceleration vs z for the cases described in Fig. 3. The units are arbitrary. Only the behavior relative to the curve S is relevant.

ues of U and $2\pi/k$, supersaturation leads to slightly greater accelerations which, however, are reached only at 2–3 km above the breaking level. The approach to the equilibrated level of acceleration is now smooth. For more extreme values of U and $2\pi/k$, the equilibrated values of acceleration are about double what one obtains in the simple model and take about 20 km to be reached. It takes about 5 km for these accelerations to exceed the values obtained with the simple model.

4. Concluding remarks

Given the simplicity of our approach, it seems unlikely that our numerical results are precise. The calculations, however, illustrate the facts that the small amount of clipping which occurs at breaking is not sufficient to completely and instantly stop wave amplitude growth, but that the energetic demands of convective motion strongly limit the degree of supersaturation that can actually occur. The illustration of the roles of both clipping and energetic consistency is the primary purpose of the present paper.

One unrealistic idealization in the present calculations is the assumption of a fixed, constant U. Clearly, as a breaking wave propagates upward, it will decelerate U, thus limiting both supersaturation and acceleration (or deceleration depending on ones frame of reference). Indeed, as U approaches zero, acceleration will disappear as the wave gets totally absorbed.

Where variations in U play an important role in determining the wave amplitude, our approach to the estimation of μ ought to be altered. However, this only occurs when U (or more generally, $U - c$) is small, in which case the present results show that there will be almost no supersaturation, and the considerations emphasized in this paper are unimportant.

Another idealization is the use of monochromatic plane waves. While this idealization is explicitly or implicitly involved in all current applications of gravity wave breaking (Holton, 1982; McFarlane, 1987; Palmer, et al., 1987 are examples), it is clear that in reality we frequently have a superposition of many waves. This is particularly clear in the case of waves excited by flow past a single mountain. The study of the breaking of such structures, while obviously important, is still in its early stages.

Finally, Lindzen (1981) dealt not only with saturation and its associated acceleration of the mean flow (gravity wave drag), but also with the turbulent diffusion arising from the convective turbulence produced by the breaking gravity waves. In Lindzen (1981), as in the present paper, the distribution of wave amplitude was calculated directly from the assumed model of breaking and equilibration. However, following Hodges (1968), Lindzen (1981) also asked what distribution of turbulent diffusion would produce this amplitude distribution, and identified this diffusion with the turbulent diffusion produced by the convective breaking of the waves. While this procedure has a certain plausibility, it is undeniably crude and speculative. Chao and Schoeberl (1984) noted that since convective breaking was associated with regions where isentropes were nearly vertical, the thermal diffusion acting on the wave will be small, and the turbulent Prandtl number appropriate to the attenuation of the wave will be large [as opposed to Pr = 1, as assumed by Hodges (1968) and Lindzen (1981)]. Since the diffusion acting on the wave is primarily momentum diffusion, a larger diffusion coefficient will be needed to produce calculated wave-amplitude distribution. This effect is diminished when wave breaking occurs over a significant portion of the wave, as is the case in the present paper when we have a significant degree of supersaturation. Chao and Schoeberl (1984) also note that the Prandtl number for the diffusion of mean quantities will be on the order of unity. This is consistent with Fig. 1c, which suggests that all isentropes are connected by the convective turbulence associated with the breaking waves. Finally, as noted by Lindzen (1984), all estimates of diffusion (and wave drag) resulting from breaking gravity waves and applied to large-scale fields must be reduced because of spatial and temporal intermittency in the wave fields (highly uncertain matters in their own right). In the present paper we have refrained from dealing with the calculation of turbulent diffusion in any detail since such calculations do not enter into the calculation of wave amplitudes resulting from wave breaking.

Acknowledgments. This work was supported by NASA Grant NAGW-525 and NSF Grant ATM-8342482. The author also thanks M. Schoeberl for numerous discussions on the topic of supersaturation of breaking waves.

APPENDIX

Convective Time Scale

In this Appendix we briefly demonstrate the origin of Eq. (7). The treatment is similar to that found in Lamb (1932). Briefly, we wish to consider the supersaturated wave plus the original basic state as a basic state for further perturbations. The equation for these perturbations will be of the form

$$\frac{d^2w'}{dz^2} + \left\{\frac{N^2}{\sigma^2} - 1\right\}k^2w' = 0$$

where

$$N^2 = \frac{g}{\bar{T}}\left[\frac{d}{dz}(\delta T + \bar{T}) + \frac{g}{c_p}\right].$$

For simplicity, take N^2 to be locally constant, and consider a region where δT is such as to render N^2 maximally negative. Solutions will exist of the form

$$w' \sim \exp[i(\sigma t + lz + kx)]$$

where

$$\sigma^2 = \frac{N^2}{1 + (l^2/k^2)}.$$

Since

$$N^2 < 0, \quad \sigma = i\sigma_c, \quad \text{and}$$

$$\sigma_c^2 = \frac{-N^2}{1 + (l^2/k^2)} \leq -N^2.$$

In terms of the notation of section 2,

$$-N^2 = \frac{g}{T}(|\tilde{A}| - 1)\Gamma,$$

and Eq. (7) follows.

REFERENCES

Chao, W. C., and M. R. Schoeberl, 1984: On the linear approximation of gravity wave saturation in the mesosphere. *J. Atmos. Sci.*, **41**, 1893–1898.

Hodges, R. R., Jr., 1969: Eddy diffusion coefficients due to instabilities in internal gravity waves. *J. Geophys. Res.*, **74**, 4087–4090.

Holton, J. R., 1982: The role of gravity wave induced drag and diffusion in the momentum budget of the mesosphere. *J. Atmos. Sci.*, **39**, 791–799.

Howard, L. N., 1961: Note on a paper of John W. Miles. *J. Fluid Mech.*, **10**, 509–512.

Lamb, H., 1932: *Hydrodynamics*, Cambridge University Press, 738 pp.

Lindzen, R. S., 1967: Thermally driven tide in the atmosphere. *Quart. J. Roy. Meteor. Soc.*, **93**, 18–42.

——, 1968: The application of classical tidal theory. *Proc. Roy. Soc.*, **A303**, 299–316.

——, 1981: Turbulence and stress due to gravity wave and tidal breakdown. *J. Geophys. Res.*, **86**, 9707–9714.

——, 1984: Gravity waves in the mesosphere. *Dynamics of the Middle Atmosphere*, J. R. Holton and T. Matsuno, Eds. Terra Scientific.

——, and D. Blake, 1971: Internal gravity waves in atmospheres with realistic dissipation and temperature: Part II. Thermal tides excited below the mesopause. *Geophys. Fluid Dyn.*, **2**, 31–61.

——, and J. Forbes, 1982: Turbulence originating from stable internal waves. *J. Geophys. Res.*, **88**, 6549–6553.

——, and J. Barker, 1985: Instability and wave overreflection in stably-stratified shear flow. *J. Fluid Mech.*, **151**, 189–217.

McFarlane, N. A., 1987: The effect of orographically excited gravity wave drag on the general circulation of the lower stratosphere and troposphere. *J. Atmos. Sci.*, **44**, (in press).

Palmer, S. N., G. J. Shutts and R. Swinbank, 1986: Alleviation of a systematic westerly bias in general circulation and numerical weather prediction models through an orographic gravity drag parameterization. *Quart. J. Roy. Meteor. Soc.*, **112**, 1001–1039.

Weinstock, J., 1987: The turbulence field generated by a linear gravity wave. *J. Atmos. Sci.*, **44**, 410–420.